Electronic Supplementary Material (ESI) for RSC Advances.

Electronic Supplementary Material (ESI)

Experimental and modelling studies of carbon dioxide capture onto pristine, nitrogen-doped and activated ordered mesoporous carbons

Talla Venkata Rama Mohan [a], Palla Sridhar [b], Parasuraman Selvam [a,c*]

[a] *National Centre for Catalysis Research and Department of Chemistry, Indian Institute of Technology-Madras, Chennai 600 036, India*

[b] *Department of Chemical Engineering, Indian Institute of Technology-Madras, Chennai 600 036, India*

[c] *International Research Organization for Advanced Science and Technology, Kumamoto University, 2-39-1 Kurokami, Kumamoto 860-8555, Japan*

*Corresponding Author. Tel.: +91 -44-2257-4235/4200 E-mail: selvam@iitm.ac.in (P. Selvam)

This PDF file includes: ESI Figures S1-S12 and Tables S1-S2

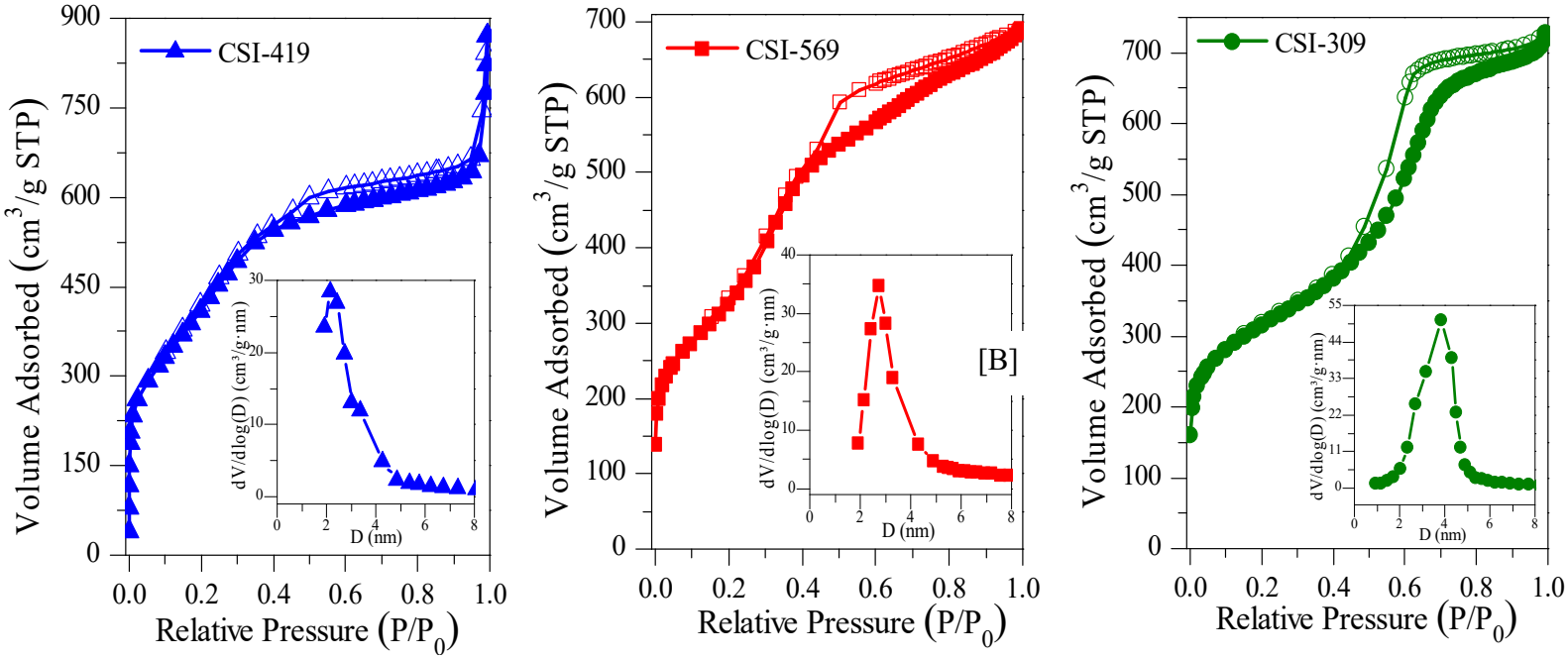

Figure S1. N_2-sorption isotherm of various 1D-hexagonal OMCs pyrolysed at 900°C. Inset: BJH pore size distribution.

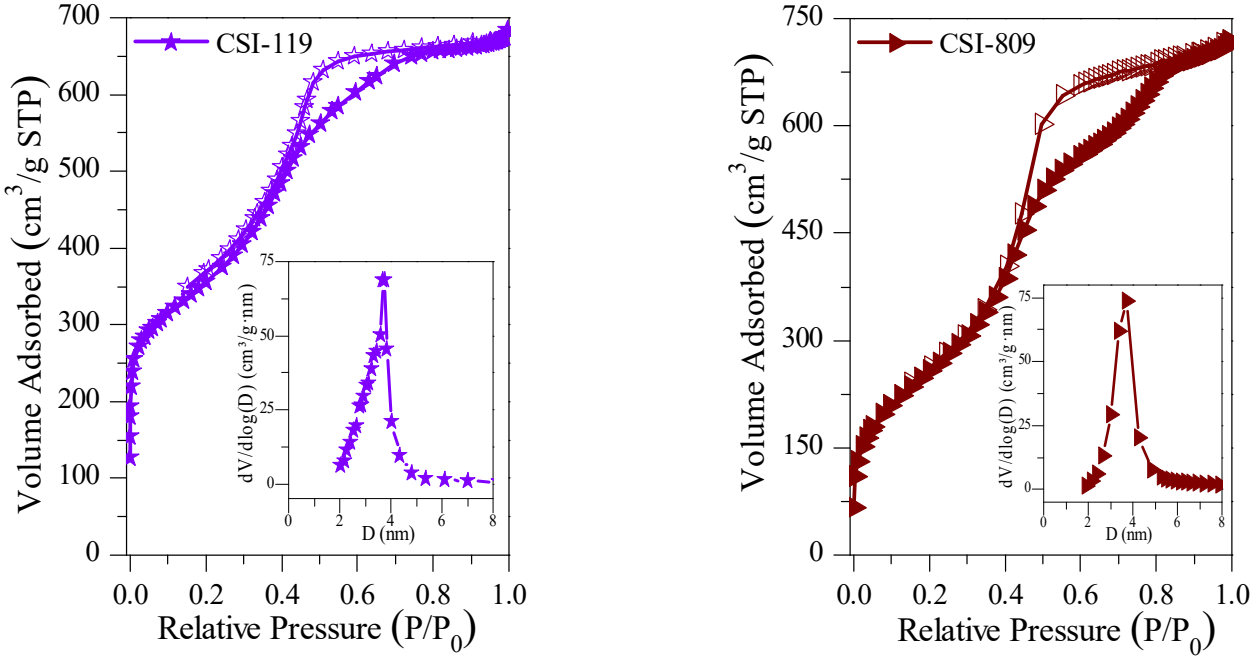

Figure S2. N_2-sorption isotherm of various 3D-cubic OMCs pyrolyzed at 900°C. Inset: BJH pore size distribution.

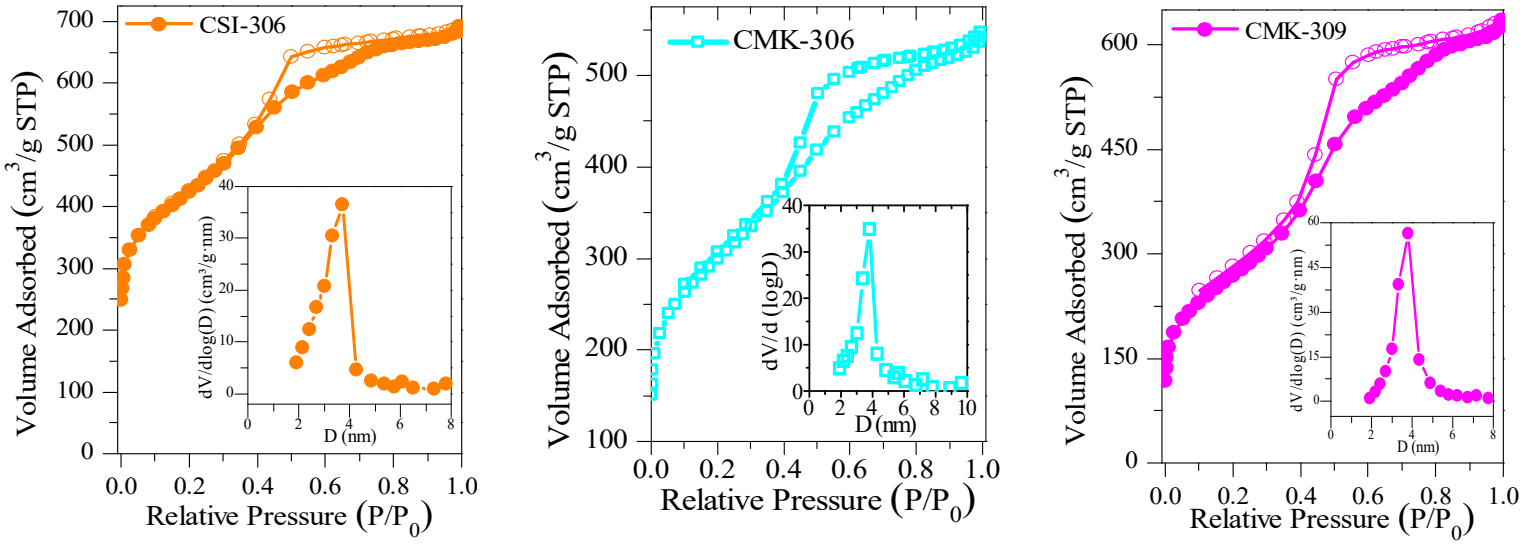

Figure S3. N_2-sorption isotherm of various 1-D hexagonal OMCs pyrolysed at 600 and 900°C. Inset - BJH pore size distribution.

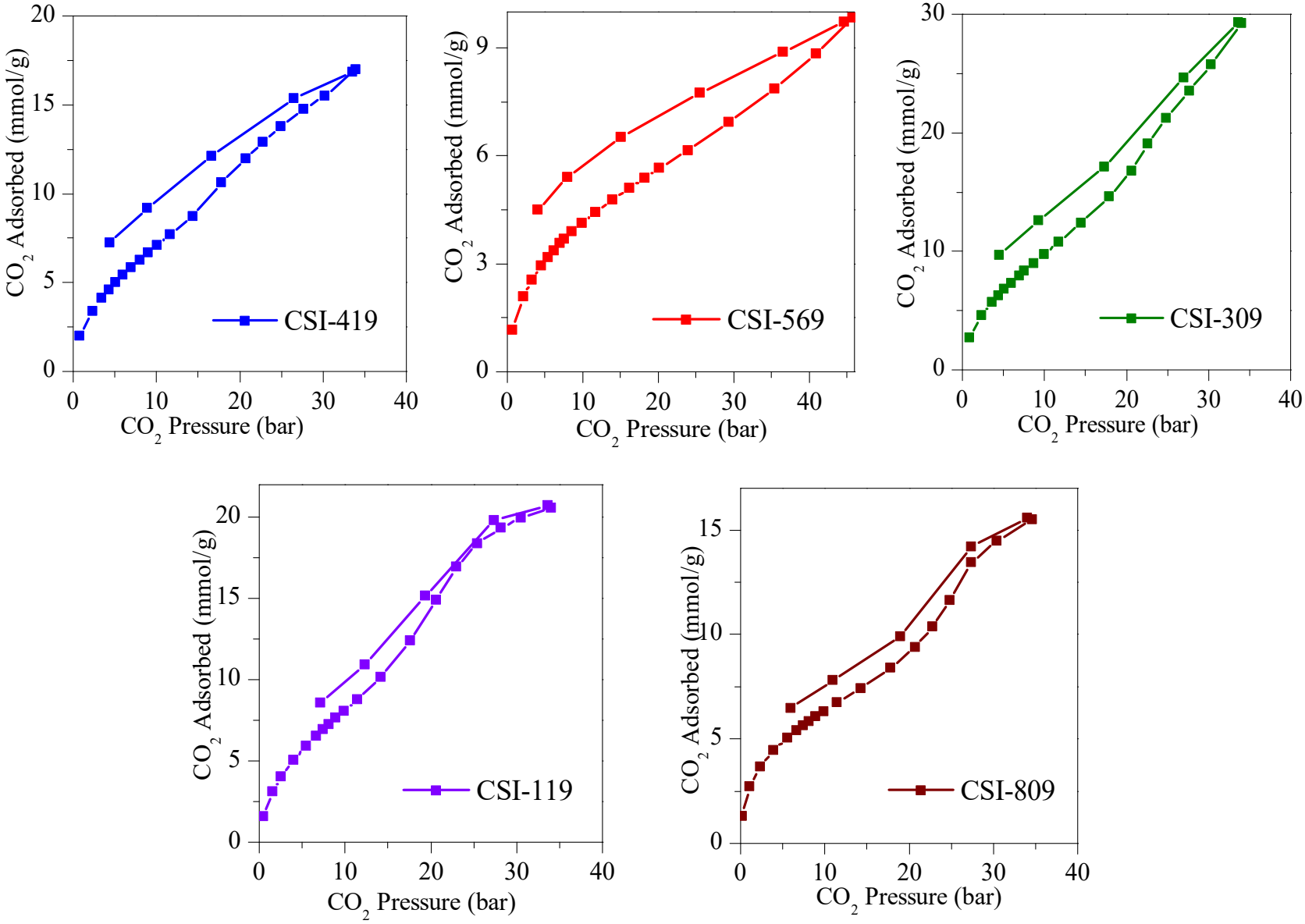

Figure S4. Experimental CO_2 adsorption-desoption isotherms at 0°C for various 1-D hexagonal and 3-D cubic OMCs pyrolyzed at 900°C.

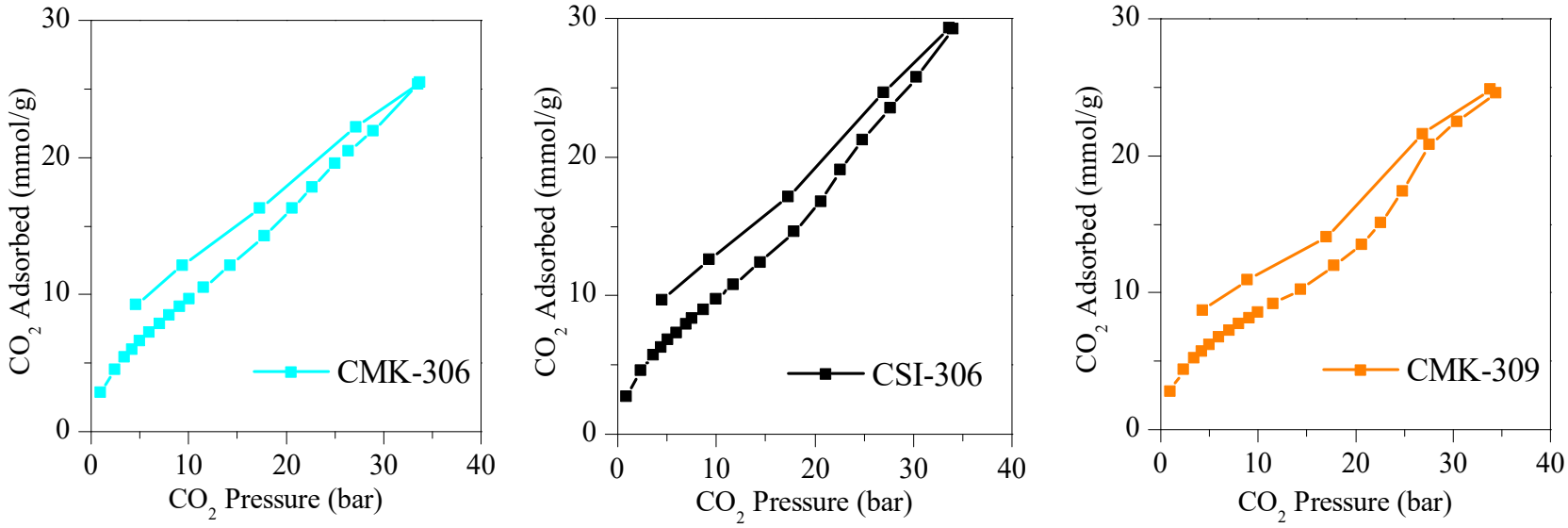

Figure S5. Experimental CO_2 adsorption-desoption isotherms measured at 0°C for various 1-D hexagonal OMCs pyrolysed at 600 and 900°C.

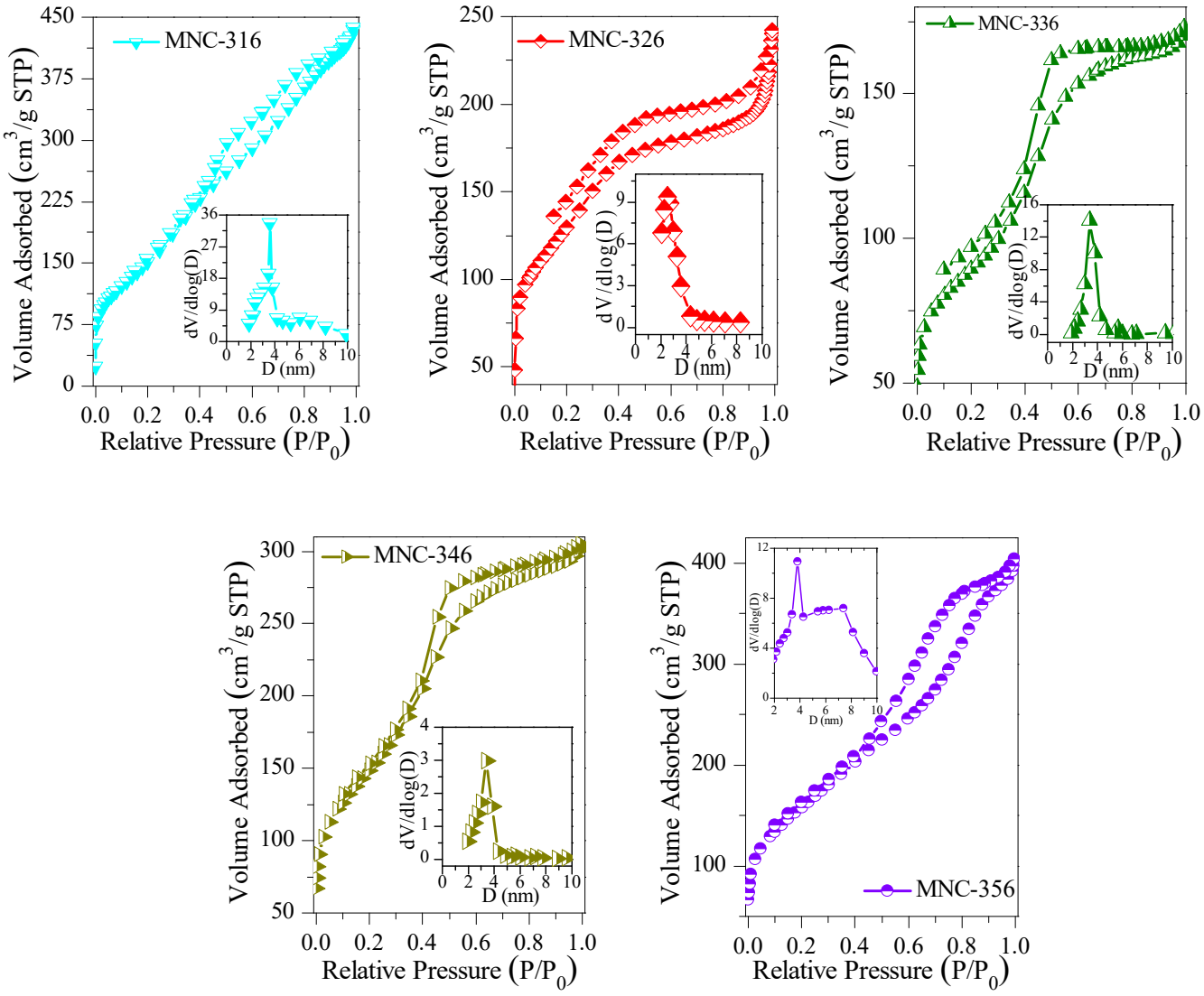

Figure S6. N_2-sorption isotherms of various 1-D hexagonal MNCs pyrolysed at 600°C. Inset: BJH pore size distributions.

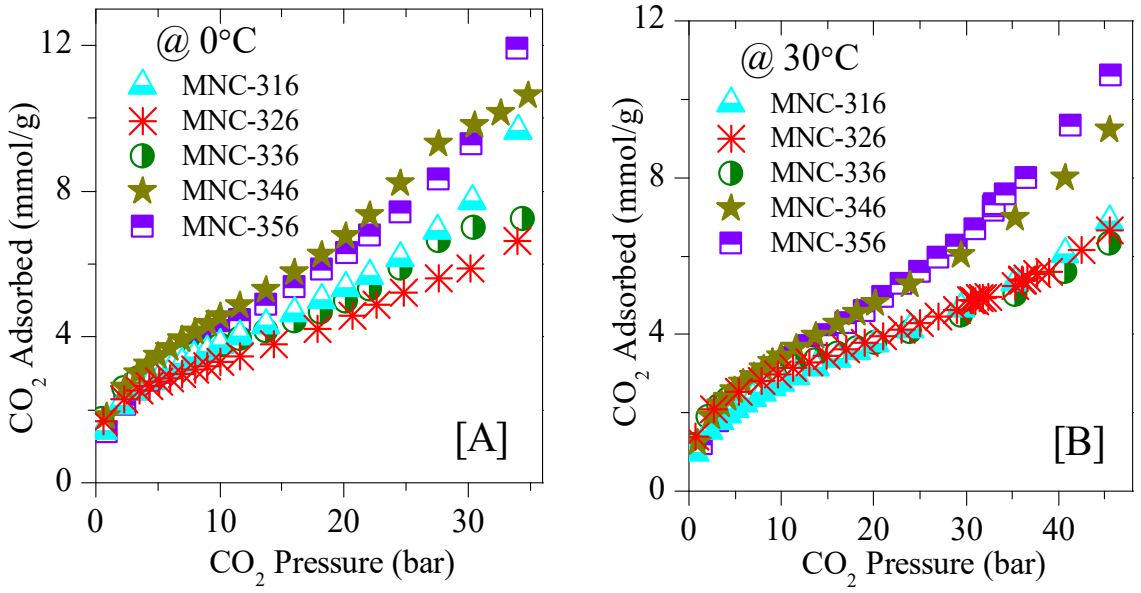

Figure S7. Experimental CO_2 excess adsorption isotherm measurements of nitrogen-doped OMCs at [A] 0°C and [B] RT.

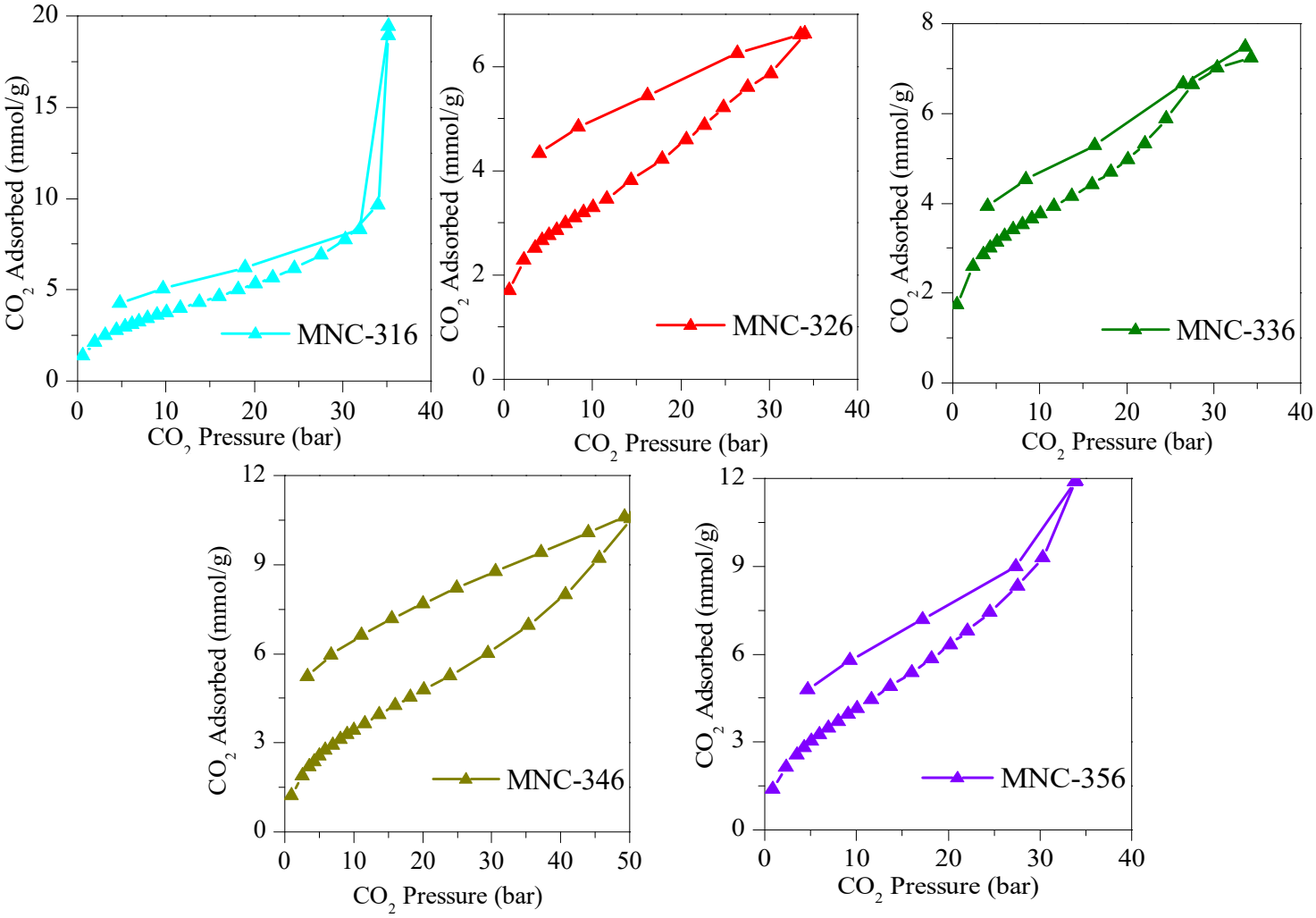

Figure S8. Experimental CO_2 adsorption-desoption isotherms measured at 0°C for various 1D-hexagonal MNCs pyrolysised at 600°C.

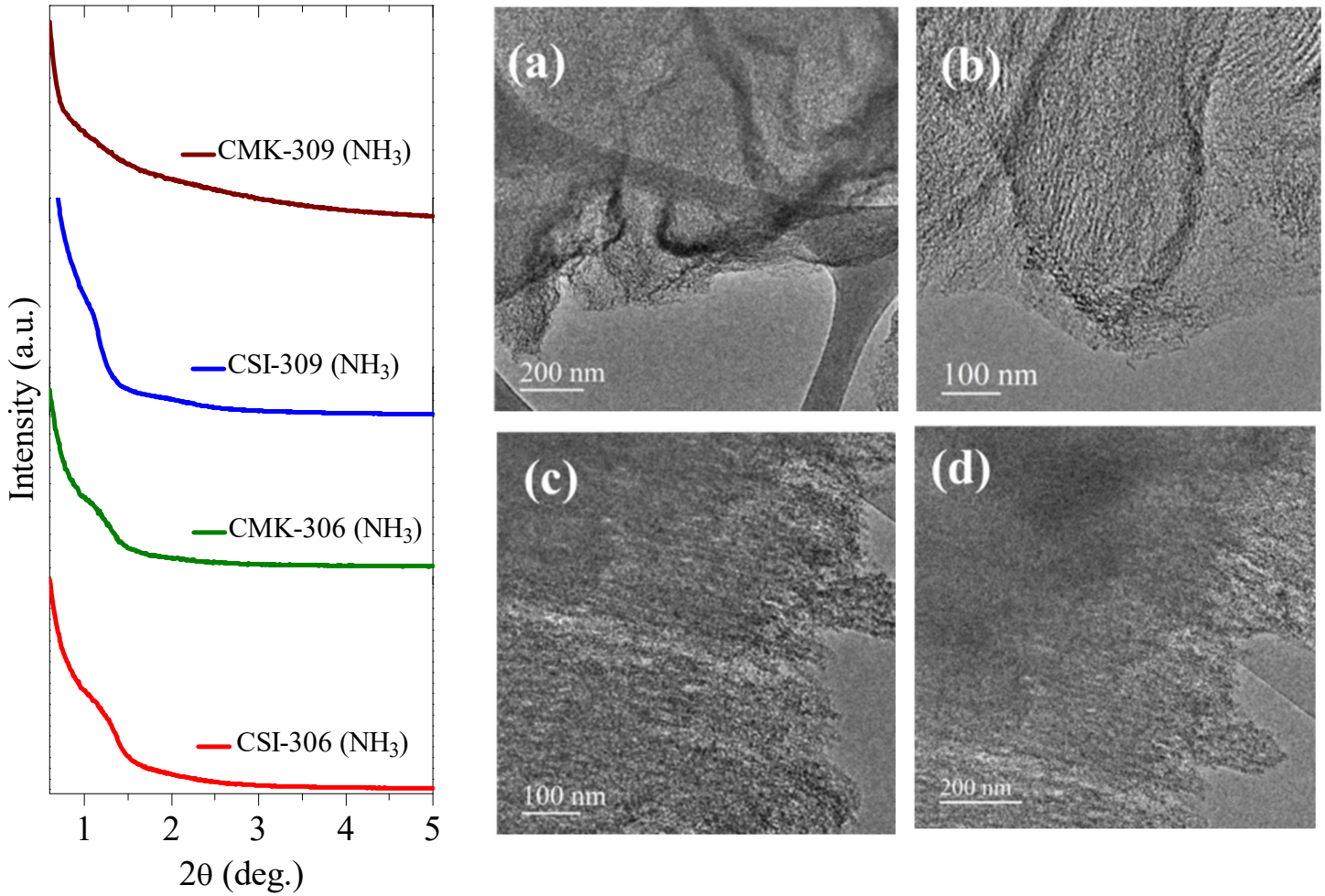

Figure S9. Low angle XRD patterns of ammonia post-synthesized carbons and HRTEM images of: (a) CSI-306 (NH_3) (b) CSI-309 (NH_3) (c) CMK-306 (NH_3) (d) CMK-309 (NH_3).

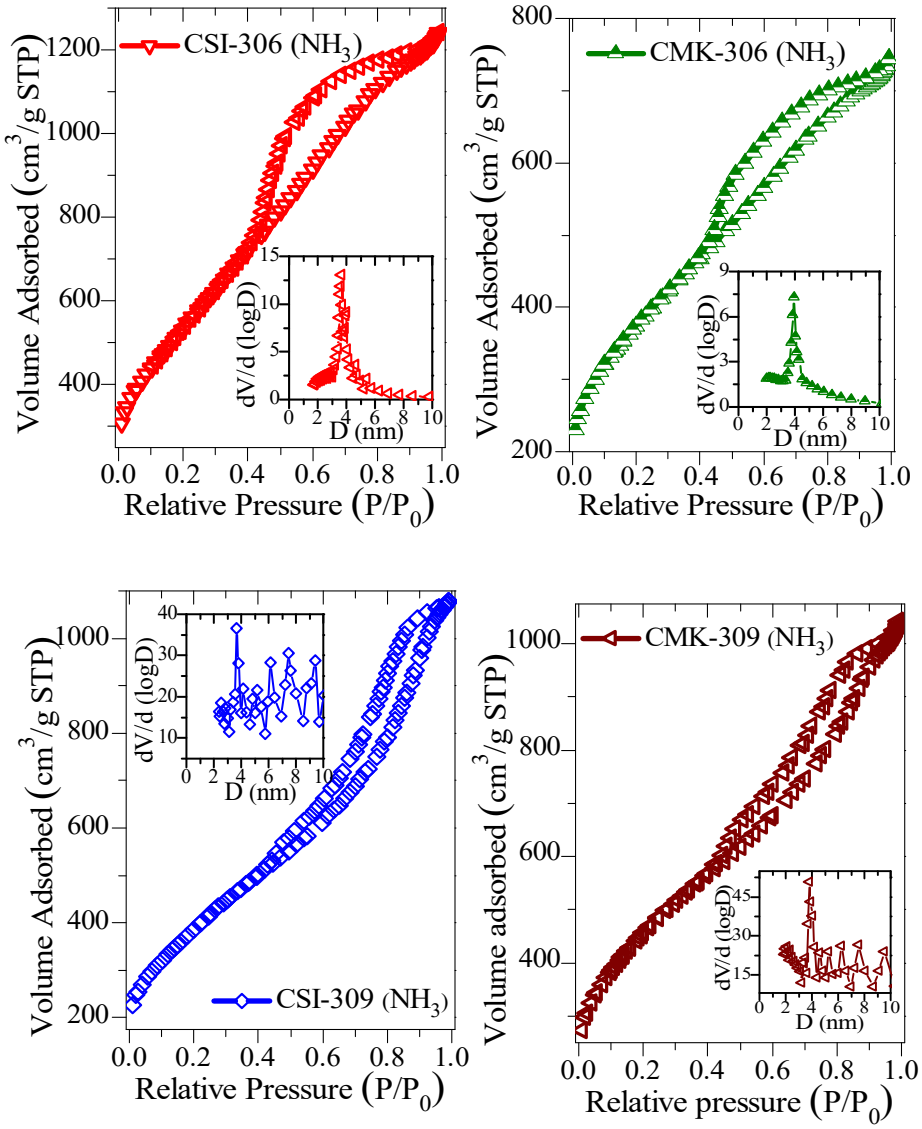

Figure S10. N_2 adsorption-desorption isotherms of ammonia-activated OMCs. Inset: BJH pore size distribution.

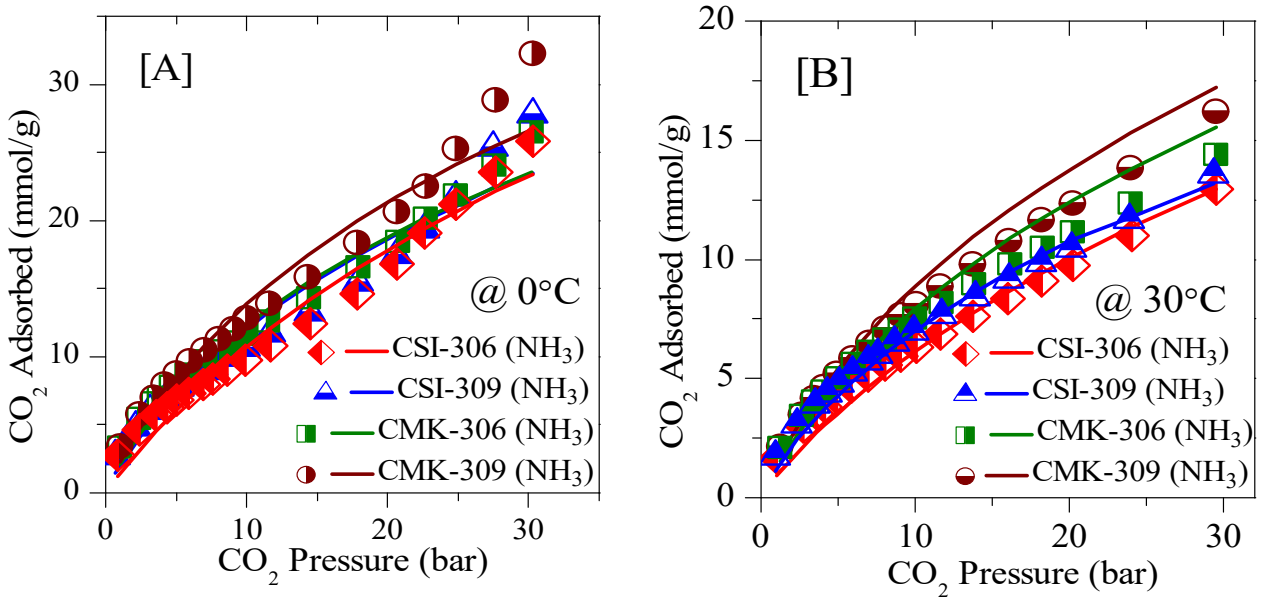

Figure S11. Experimental CO_2 excess adsorption isotherm measurements (solid symbols) and modified Toth fit (solid lines) of ammonia-activated carbons at [A] 0°C and [B] RT.

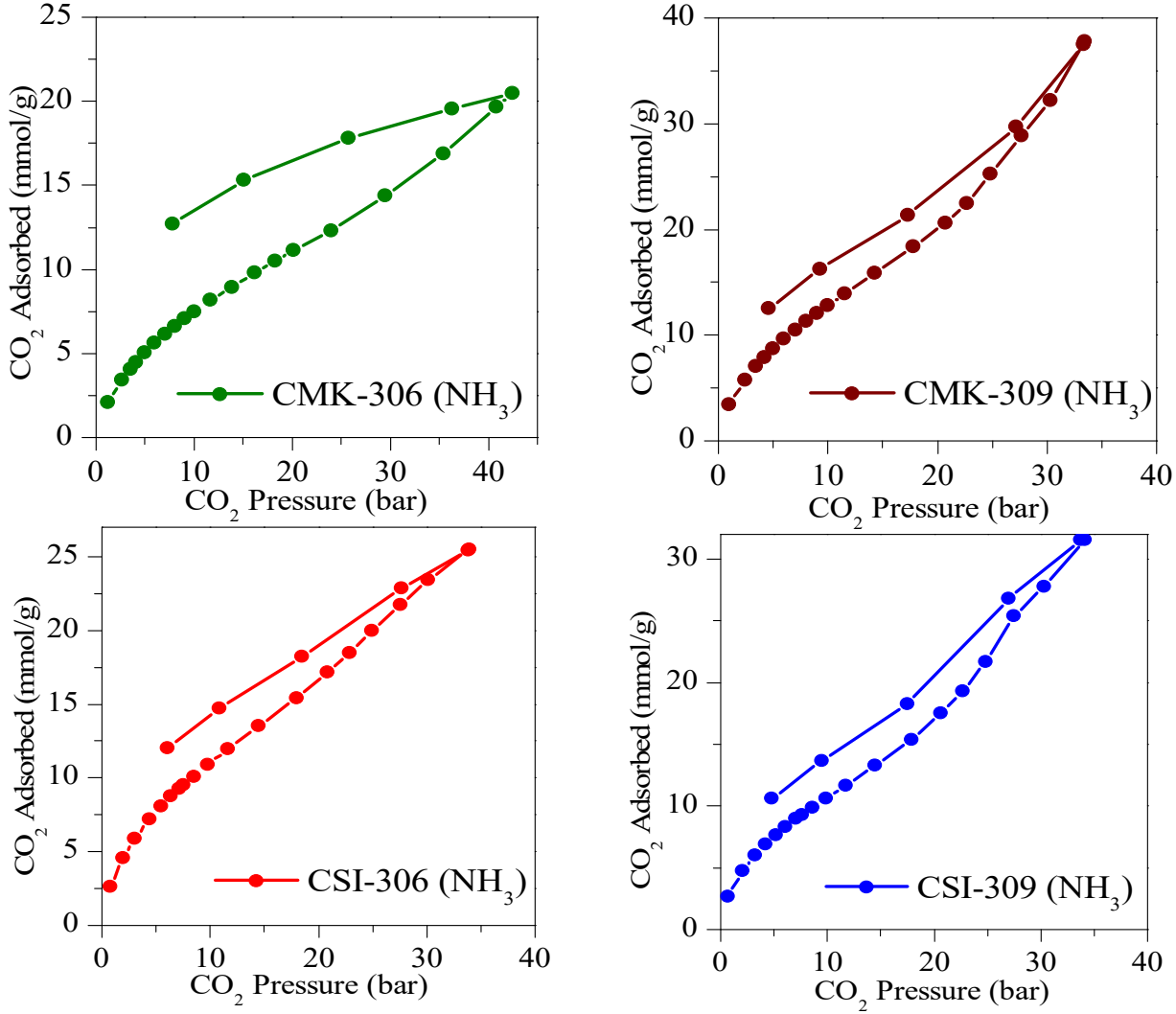

Figure S12. Experimental CO_2 adsorption-desorption isotherms measured at 0°C for various ammonia-activated 1D-hexagonal OMCs.

Table S1. Literature review on carbon dioxide storage on various porous carbon materials.

Adsorbent	Template	Source	S_{BET} (m^2g^{-1})	V_p (cm^3g^{-1})	N (*at %*)	CO_2 uptake, *mmol/g* (*bar*)		Ref.
						25℃	0℃	
Ordered mesoporous carbons								
CMK-3	SBA-15	Sucrose	970	0.81	--	2.4 (1)	3.2 (1)	[1]
CMK-3	SBA-15	Sucrose	1491	1.34	--	6.4 (10)	--	[2]
CMK-3	SBA-15	Sucrose	1115	1.15	--	18.6 (35)	--	[3]
CMK-3-150	SBA-15-mw	Sucrose	1205	1.46	--	--	24.4 (30)	[4]
CMK-3	SBA-15	Sucrose	1491	1.30	--	14.6 (40)	--	[5]
CMK-8	KIT-6	Sucrose	1020	0.91	--	2.1 (1)	--	[1]
EPC-1	EPG-1	Sucrose	1551	1.41	--	--	26.3 (30)	[6]
Nitrogen-doped porous carbons								
PVA-CMK-3	CMK-3	N-vinylformamide/AIBN	711	0.46	--	3.5 (1)	--	[7]
CS-6-CD-4	Silica sphere	Resorcinol/HCHO/NH_3	661	0.30	--	2.5 (1)	--	[8]
NMC-M/P-0.5	LudoxSM-30	Melamine/Phenol/HCHO	777	2.3	4.3	1.5 (1)	2.0 (1)	[9]
Meso-CN	MCF	Ethylenediamine/CCl_4	502	2.30	17.8	2.5 (1)	--	[10]
RFL-500	--	Resorcinol/HCHO	467	0.23	1.9	3.1 (1)	--	[11]
MF-700	MCM-41 type	Melamine/Methanol/HCHO /Borax/K_2CO_3	266	0.25	21	0.8 (1)	--	[12]
NOMC-800	F127	Urea/Phenol/Resorcinol	645	0.36	2.4	2.5 (1)	3.3 (1)	[13]
NOMC-0.1	F127	Urea/Phenol/HCHO	566	0.31	0.9	2.4 (1)	--	[14]
NOMC-700	SBA-15	Ethylviolet/Sulfuric acid	959	1.49	12.9	8.8 (30)	18.1 (30)	[15]

Adsorbent	Template	Source	S_{BET} (m^2g^{-1})	V_p (cm^3g^{-1})	N (*at %*)	CO_2 uptake, *mmol/g* (*bar*)		Ref.
						25℃	0℃	
MCN-1	SBA-15	Ethylenediamine/CCl_4	738	0.92	6.2	9.1 (30)	20.1 (30)	16], [17]
MNC-7	FDU-12	Ethylenediamine/CCl_4	901	1.02	19.0	5.9 (30)	13.5 (30)	[18]
IBN9-NC	IBN-9	*p*-diaminobenzene	890	0.68	18.8	5.2 (8)	--	[19]
PAC-800	SBA-15	*3*-aminobenzoic acid	1137	1.28	6.3	2.0 (1)	5.04 (1)	[20]
MCN-8E-150‡	KIT-6	*3*-amino-1,2,4-triazole	232	3.50	61.0	1.5 (30)	5.6 (30)	[16]
Physically activated carbons (CO_2)								
CS-6-CD-4	Silica spheres	Resorcinol/HCHO/NH_3	2284	0.89	--	4.5 (1)	8.05 (1)	[8]
MFZ-700	MCM-41 type	Melamine/Methanol/HCHO /Borax/K_2CO_3	193	0.32	22.7	0.9 (1)	--	[21]
Chemically activated carbons (KOH)								
ATS-2-700	SBA-15	Sucrose	1330	0.73	--	3.3 (1)	5.8 (1)	[1]
ATK-4-800	KIT-6	Sucrose	2660	1.38	--	3.1 (1)	5.4 (1)	[1]
NOMC-0.1	F127	Urea/Phenol/HCHO	1790	0.94	--	4.3 (1)	--	[14]
NOMC-800	F127	Melamine/Resorcinol/HCHO	1413	0.72	--	4.6 (1)	3.1 (1)	[13]
PIF-6	CTAB	Indole/Ammonium persulphate	527	0.20	4.1	2.9 (1)	3.2 (1)	[22]
IBN9-NC1-A	IBN-9	*p*-diaminobenzene/Furfuryl alcohol	1181	0.73	12.9	10.5 (8)	--	[19]
NPC-650	--	*m*-diaminobenzene	1561	0.75	4.1	3.1 (1)	5.3 (1)	[23]

‡*g*-C_3N_4 ; §At 30℃.

Table S2. Modeling parameters for carbon dioxide storage on various mesoporous carbon materials.

Adsorbent	Toth model fitting parameters						CO_2 uptake, *mmol/g*	
	$b_0 \times 10^{-8}$	n_{max}	Q	t_0	α	R^2	30°C (45 bar)	0°C (34 bar)
CSI-809	6.6	70.8	4001	0.38	-0.51	0.95	10.7	15.5
CSI-119	3.54	76.4	4004	0.60	-1.74	0.97	14.8	20.7
CSI-419	2.80	48.12	5077	0.66	-1.80	0.98	13.3	16.9
CSI-569	5.87	64.7	4008	0.41	-0.79	0.97	9.8	13.2
CSI-309	5.86	99	7768	0.524	-0.73	0.97	17.8	25.4
CMK-309	5.25	86	8100	0.57	-0.89	0.94	14.4†	24.4
CSI-306	6.75	89.24	7242	0.724	-2.17	0.97	22.5	27.5
CMK-306	5.30	83.5	8291	0.6	-0.79	0.95	16.3	25.4
CSI-306 (NH_3)	2.39	65.8	13148	0.45	-0.44	0.95	20.8	29.3
CSI-309 (NH_3)	1.60	85.9	6422	0.57	-1.40	0.95	21.5	31.5
CMK-306 (NH_3)	5.22	84.2	9175.88	0.56	-0.72	0.97	16.6	29.0
CMK-309 (NH_3)	1.42	89.94	6912.09	0.59	-1.03	0.95	23.1	37.8
MNC-316	2.20	94.72	4008.3	0.21	-0.16	0.96	6.9	9.6
MNC-326	3.08	45.25	15207	0.17	0.04	0.94	6.6	6.7
MNC-336	1.39	40.37	15052	0.208	-0.017	0.93	6.3	7.3
MNC-346	8.50	99	9423.16	0.26	-0.13	0.95	9.2	10.4
MNC-356	1.25	61.4	6837.77	0.36	-0.27	0.95	10.6	11.9

Table S3. Structural and textural properties of various 1-D hexagonal and 3-D cubic ordered mesoporous silicas [24].

Hard (OMS) templates	a_0 $(nm)^{\dagger}$	S_{BET} $(m^2g^{-1})^{\ddagger}$	V_p $(cm^3g^{-1})^{\S}$	D_{BJH} $(nm)^{\P}$	D_{TEM} $(nm)^{\$}$
MCM-41	4.2	966	0.86	2.5	2.6
IITM-56	6.0	758	0.89	3.8	3.6
SBA-15	10.1	576	0.96	6.4	6.5
SBA-11	13.7	671	0.69	1.9	2.1
KIT-6	20.0	785	1.07	6.8	6.7

†For hexagonal system: $a_0 = 2d_{100}/\sqrt{3}$. For cubic system: $a_0 = d \times (h^2+l^2+k^2)^{1/2}$. $^{\ddagger}S_{BET}$ = Surface area calculated using BET equation. $^{\S}V_P$ = Total pore volume. $^{\P}D_{BJH}$ = Pore size determined using BJH method. $^{\$}D_{TEM}$ = Pore size determined using TEM.

References

1. M. Sevilla and A. B. Fuertes, *Journal of Colloid and Interface Science*, 2012, **366**, 147-154.
2. C.-C. Huang and S.-C. Shen, *Journal of the Taiwan Institute of Chemical Engineers*, 2013, **44**, 89-94.
3. J. Zhou, W. Su, Y. Sun, S. Deng and X. Wang, *Journal of Chemical & Engineering Data*, 2016, **61**, 1348-1352.
4. K. S. Lakhi, W. S. Cha, J.-H. Choy, M. Al-Ejji, A. M. Abdullah, A. M. Al-Enizi and A. Vinu, *Microporous and Mesoporous Materials*, 2016, **233**, 44-52.
5. G. Chandrasekar, W.-J. Son and W.-S. Ahn, *Journal of Porous Materials*, 2009, **16**, 545-551.
6. Y.-R. Pei, G. Choi, S. Asahina, J.-H. Yang, A. Vinu and J.-H. Choy, *Chemical Communications*, 2019, **55**, 3266-3269.
7. C.-C. Hwang, Z. Jin, W. Lu, Z. Sun, L. B. Alemany, J. R. Lomeda and J. M. Tour, *ACS Applied Materials & Interfaces*, 2011, **3**, 4782-4786.
8. N. P. Wickramaratne and M. Jaroniec, *ACS Applied Materials & Interfaces*, 2013, **5**, 1849-1855.
9. H. Chen, F. Sun, J. Wang, W. Li, W. Qiao, L. Ling and D. Long, *The Journal of Physical Chemistry C*, 2013, **117**, 8318-8328.
10. Q. Li, J. Yang, D. Feng, Z. Wu, Q. Wu, S. S. Park, C.-S. Ha and D. Zhao, *Nano Research*, 2010, **3**, 632-642.
11. G.-P. Hao, W.-C. Li, D. Qian and A.-H. Lu, *Advanced Materials*, 2010, **22**, 853-857.
12. C. Goel, H. Bhunia and P. K. Bajpai, *RSC Advances*, 2015, **5**, 46568-46582.
13. J. Yu, M. Guo, F. Muhammad, A. Wang, F. Zhang, Q. Li and G. Zhu, *Carbon*, 2014, **69**, 502-514.
14. A. Chen, Y. Yu, Y. Zhang, W. Zang, Y. Yu, Y. Zhang, S. Shen and J. Zhang, *Carbon*, 2014, **80**, 19-27.
15. S. Zhou, H. Xu, Q. Yuan, H. Shen, X. Zhu, Y. Liu and W. Gan, *ACS Appl. Mater. Interfaces*, 2016, **8**, 918-926.
16. D.-H. Park, K. S. Lakhi, K. Ramadass, M.-K. Kim, S. N. Talapaneni, S. Joseph, U. Ravon, K. Al-Bahily and A. Vinu, *Chemistry – A European Journal*, 2017, **23**, 10753-10757.
17. K. S. Lakhi, A. V. Baskar, J. S. M. Zaidi, S. S. Al-Deyab, M. El-Newehy, J.-H. Choy and A. Vinu, *RSC Advances*, 2015, **5**, 40183-40192.
18. K. S. Lakhi, W. S. Cha, S. Joseph, B. J. Wood, S. S. Aldeyab, G. Lawrence, J.-H. Choy and A. Vinu, *Catalysis Today*, 2015, **243**, 209-217.

19. Y. Zhao, L. Zhao, K. X. Yao, Y. Yang, Q. Zhang and Y. Han, *Journal of Materials Chemistry*, 2012, **22**, 19726-19731.
20. Á. Sánchez-Sánchez, F. Suárez-García, A. Martínez-Alonso and J. M. D. Tascón, *ACS Applied Materials & Interfaces*, 2014, **6**, 21237-21247.
21. D. Tiwari, C. Goel, H. Bhunia and P. K. Bajpai, *Journal of Environmental Management*, 2017, **197**, 415-427.
22. M. Saleh, J. N. Tiwari, K. C. Kemp, M. Yousuf and K. S. Kim, *Environmental Science & Technology*, 2013, **47**, 5467-5473.
23. J. Wang, I. Senkovska, M. Oschatz, M. R. Lohe, L. Borchardt, A. Heerwig, Q. Liu and S. Kaskel, *Journal of Materials Chemistry A*, 2013, **1**, 10951-10961.
24. T.V.R. Mohan, PhD Thesis, IIT-Madras, 2021.